Improving Communication Performance of Passive Backscattering Tags Using Collaborative Backscatter

Abeer Ahmad,* Manavjeet Singh,* Yang Xie,◇ Xiao Sha,◇ Milutin Stanaćević,◇
Samir R. Das,* and Petar M. Djurić◇
*Department of Computer Science, Stony Brook University, Stony Brook, NY, USA
◇ Department of Electrical and Computer Engineering, Stony Brook University, Stony Brook, NY, USA

***Abstract*—We propose collaborative backscatter techniques for tag-to-tag communication between battery-less RF tags. The low incident backscatter power and the limited processing ability in the passive receive circuits limit the performance of such links. By recruiting 'helper' tags to boost backscatter signals, such links can be substantially strengthened, depending upon the network topology and channel conditions. Two techniques are developed and evaluated on a prototype tag network, demonstrating close-to-optimal performance with low computational overhead.**

I. Introduction

In conventional backscatter-based systems the receive side of the backscatter link relies on an active (battery or externally powered) receiver, e.g., the 'reader' in an RFID system. Such receivers have significant signal processing ability and can employ IQ demodulation and carrier cancellation resulting in a high sensitivity. However, making active receivers a critical part of the system limits scalability and ubiquitous deployment. In this work, we are specifically interested in a network of 'passive' RF tags that can run on harvested power alone and can backscatter an external signal to *communicate directly among themselves.* Such tags need to be able to both transmit and receive without specifically relying on active transceivers. The external signal can be *ambient* [1] (if suitable signals with enough power are available) or an intentionally generated RF signal through a dedicated 'exciter' [2].

This tag-to-tag communication enables scalable IoT networks where everyday objects are interconnected, with active devices limited to gateways to external networks. Such a vision has encouraged a line of research in recent years studying and developing tag-to-tag communication with passive tags [3], [1], [4], [2], [5], [6].

A major challenge in tag-to-tag communication is the weak backscatter signal due to the limited sensitivity of passive demodulation techniques employed on receiver tags [2], [7]. This restricts communication range (a few meters) and data rates (a few kbps), impacting connectivity in sparse networks and creating bottlenecks in multihop routing. Such bottlenecks strain the energy budgets of tags, as processing consumes significant power [8]. Enhancing connectivity and link robustness is essential for reliable deployment in practical applications.

We address connectivity challenges by introducing a signal-boosting mechanism using nearby 'helper' tags, which otherwise remain idle. Two techniques are developed: in the first, helper tags adjust their reflection phases to boost backscatter signals, similar to [9]. In the second, helper tags proactively transmit the same data with symbol-specific phases to enhance the intended signal similar to our preliminary studies in [10]. While finding optimal helper configurations via exhaustive search is computationally expensive, we demonstrate that heuristic methods achieve near-optimal performance efficiently. These heuristics are evaluated on a 7-node tag testbed using a continuous wave (CW) exciter. The approach can also extend to ambient excitation sources, given sufficient RF signal power.

II. Collaborative Backscatter Techniques

The basis of our work is the ability of the 'helper' tags to influence the excitation signal at various points in space. By adjusting their reflection properties (amplitude and phase), helper tags can modify the excitation signal via constructive or destructive interferences.

The tags use PSK modulation, where the backscattering tag alters the phase of the reflected signal to represent bits "0" and "1." At the receiving tag, this signal combines with the CW excitation signal from the exciter, producing two distinct resultant signals. The envelope detector extracts the signal amplitude, and the difference between these amplitudes — known as 'modulation depth' — determines link performance. A larger modulation depth increases the separation between amplitude levels, reducing bit error rate (BER) and enhancing link robustness [11], [12]. Since BER is exponentially dependent on modulation depth, even small improvements n modulation depth significantly enhance performance. Better BER supports higher bit rates and longer communication distances. In this work, we do not directly evaluate the BER, bit rate, or link length. Instead, we focus on modulation depth as a proxy for these metrics.

We propose two techniques that use otherwise idle helper tags to improve link quality. These helpers strategically adjust their reflection phases to enhance communication between a transmitter-receiver pair. Although this paper focuses on optimizing a single link, the methods can potentially scale to multiple links (Section II-D).

A. Scheme 1: Passive Reflection by Helper Tags

In this technique, a suitable subset of tags is designated as 'helper' tags, each helper tag k setting its reflection coefficient Γ_k to a specific value from a predefined set. The goal is to

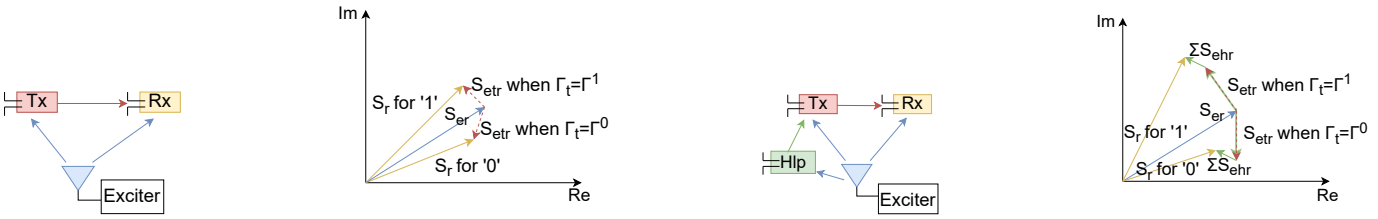

(a) Schematic (b) Signal phasors at receiver (c) Schematic (d) Signal phasors at receiver

Fig. 1: Overview of Scheme 1: (a) and (b) show the baseline case with no helpers, (c) and (d) depict the case with one helper tag.

boost the transmitter's signal and significantly improve modulation depth over the baseline (no helpers). Once configured, the helper tags act as passive reflectors, requiring no energy or further adjustments.

In Figure 1, the baseline scenario (subfig. a) shows no helper tags. Subfig. b shows the phasor diagrams, where sinusoidal signals are represented as stationary vectors. The excitation signal (S_{er}, blue) combines with two reflected signals from Tx (S_{etr}, red) for bits "0" and "1," respectively. The resultant signals (S_r, yellow) represent the modulation depth, defined by the amplitude difference between the two states. To maximize the modulation depth, the Tx reflection phases must align one red phasor constructively with the blue signal and the other destructively. When a helper is introduced (subfig. c), its reflected signal combines with the original excitation. If the helper's phase is set correctly, the combined signal maintains the original phase but with a higher amplitude. As a result, the reflected signal (S_{etr}) also achieves a higher amplitude (displayed by the red/green phasor, shown in subfig. d). The design goal is to optimize the helper and Tx reflection phases to maximize the difference between the two resultant S_r phasors (yellow) for bits "0" and "1", achieving a modulation depth significantly higher than the baseline modulation.

In practice, there are some limitations. The above description ignores higher-order reflections such as reflections between helper tags or reflections from Tx going into helpers. However, such reflections typically have very low power. Our experimental evaluations capture all the reflections. Second, the tags typically offer fewer than 10 reflection coefficients, constrained by RF switch ports. Thus, the specific reflection phase needed for the desired impact may not be available. Third, the backscattered signal strength is not always uniform across different phases. Nevertheless, within a specific topology, it is typically possible to identify a suitable selection of reflection coefficients for a set of helper tags that enhances the modulation depth of a given tag-to-tag link. The next section is devoted to how to find an optimal selection.

B. Selection of Reflection Coefficients on Helper Tags

An exhaustive search can identify the optimal set of reflection coefficients, but it is impractical for a large network. The total number of configurations grows exponentially as m^n, where n is the number of helper tags and m is the number of reflection coefficients per tag. So, we use a heuristic modeling and estimation approach to approximate the optimal configuration with significantly fewer measurements. It is assumed that the transmitter and helpers can communicate with the receiver, either directly or via a multi-hop route. This assumption is needed even in exhaustive search scenarios. The multi-hop assumption is especially relevant when collaborative backscatter is used to establish a direct link between tags that would otherwise suffer from a high bit error rate (BER). In such cases, modulation depth measurements may not always be directly communicated between tags. Additionally, we assume that the transmitter can communicate with all helper tags. This is reasonable, as helpers are typically located near the transmitter, making them well-positioned to enhance the backscatter signal effectively.

The proposed approach models all communication signals as phasors. For this, the amplitudes and phases of the wireless channels must be estimated. Known techniques [13], [6] allow the estimation of the amplitude and phase of tag-to-tag channels through a series of measurements proportional to the number of reflection coefficients. These measurements, performed once, unless the tags move or the environment changes significantly, are used to fit a mathematical model.[1] However, these techniques yield phase wrapping between $0-\pi$ instead of the required $0-2\pi$, which must be resolved. Additionally, there are no existing techniques for estimating the exciter-to-tag channel amplitude and phase, which presents an additional challenge.

We develop a mathematical model to calculate modulation depth for a given set of parameters, such as helper selection and reflection coefficients (see the Appendix). Known parameters, including reflection coefficients and tag-to-tag channel amplitudes and phases, are instantiated using existing techniques. However, several parameters remain unknown. To estimate them, we use a limited set of modulation depth measurements as training data and apply a nonlinear least squares curve-fitting method via Scipy's curve_fit function [15]. Around 50 direct measurements are performed for specific helper and reflection coefficient configurations, and the model estimates modulation depth for all other combinations. Importantly, our goal is to identify the optimal configuration, not to precisely estimate modulation depth. As

[1]Such measurements have broader applications in tag networks [13], [14] and are not exclusive to collaborative backscattering.

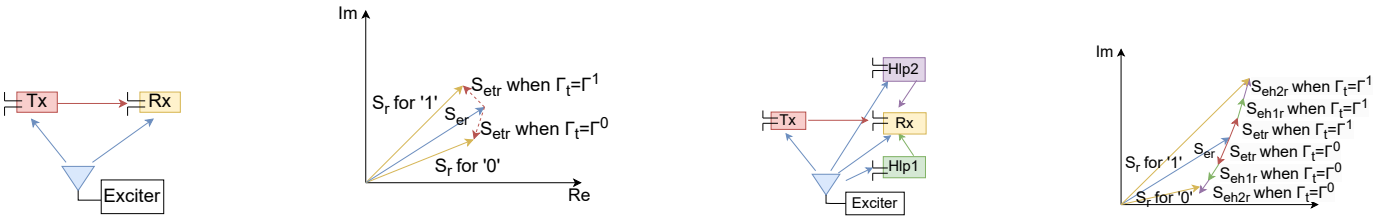

(a) Schematic (b) Signal phasors at receiver (c) Schematic (d) Signal phasors at receiver

Fig. 2: Overview of Scheme 2: (a) and (b) show the baseline case with no helpers, (c) and (d) show the case with one helper tag.

demonstrated later, this heuristic approach effectively achieves near-optimal results in practice.

C. Scheme 2: Synchronous Changes in Reflection by Helper Tags

Scheme 1 does not need any active engagement from helper tags. In contrast, in Scheme 2, helpers actively enhance the modulation depth by backscattering signals that constructively align with the receiver signal for bit '1' and destructively for bit '0'. In Figure 2, subfigures (a) and (b) illustrate the baseline scenario and phasor diagram without helpers. Subfigures (c) and (d) show the signal paths and corresponding phasor diagram with helpers. At the receiver, the exciter signal (S_{er}) combines with the backscattered signals from the transmitter (S_{etr}) and helper tags (S_{eh1r}, S_{eh2r}). While two helper tags are shown, more can be included. When the reflection phases of the transmitter and helpers are optimally aligned, they constructively add for bit '1' and destructively negate for bit '0'. As a result, the resultant signal (S_r) exhibits a significantly enhanced amplitude difference between bits '0' and '1' compared to the baseline scenario without helpers. In this description, similar to Scheme 1, we have ignored higher-order reflections due to their very low relative power. However, our experimental evaluation is real and includes all possible reflections.

Our goal is to find settings of reflection coefficients (for both bits '1' and '0') for helper tags such that the modulation depth is substantially improved. A simple heuristic as described below works well: For each tag from the set of tags SH that includes the transmitter S and all helpers $H_1, \ldots, H_n$ (i.e., $SH = \{S, H_1, \ldots, H_n\}$), the optimal reflection coefficients for the maximum modulation depth is *independently* estimated. To do this, all tags except the one (say, tag $T_k \in SH$) involved in this estimation is set in a non-reflecting state. Then, the optimal reflection coefficients for T_k are estimated by

1) measuring the voltage at the output the envelope detector of the Rx for all m reflection coefficients $\Gamma_k^i, i = 1, \ldots, m$, available on tag T_k, and then,
2) determining the coefficients, $\Gamma_k^{(1)}$ and $\Gamma_k^{(0)}$, responsible for producing the maximum and minimum voltages, respectively.

This process is repeated for all tags T_k in set SH. We note that this simple process is not effective for scheme 1 presented earlier.

For n helper tags and m reflection coefficients available on each tag, this amounts to $(n+1)m$ measurements. If we ignore the influence of the signal in the exciter-helper-Tx-Rx or exciter-Tx-helper-Rx paths (assumption ii above), then when all the tags T_k in the set SH set their reflection coefficients at $\Gamma_k^{(1)}$ and $\Gamma_k^{(0)}$ together synchronously, the respective phasors are generally expected to line up as shown (Figure 2(d)) adding constructively to the excitation signal for bit '1' and negating the excitation for bit '0'. This significantly enhances the modulation depth.

D. Discussion

1) Scheme 1: It is instructive here to qualitatively evaluate the two schemes. Scheme 1 is fully passive – helpers require no energy consumption once their reflection coefficients are set. Helpers closer to Tx provide a stronger signal boost, while distant helpers have reduced impact due to longer exciter-helper-Tx paths. Overall, Scheme 1's performance gain is modest, as signals undergo two backscatter reflections before reaching the receiver.

2) Scheme 2: In contrast, Scheme 2 requires active participation from helpers, adjusting their reflection coefficients for each bit, similar to the transmitter. This approach consumes more energy but offers a significant boost in modulation depth. This is because the signal reflects only once (at helpers), flips direction for bits '0' and '1' via phase adjustments. This scheme is most effective when the helpers are close to the Rx.

A limitation of Scheme 2 is the need for synchronous transmission, requiring the helpers to stay within the Tx's communication range to decode transmitted bits. Simple synchronization protocols can address this, such as helpers listening to backscattered bits and adjusting their reflection coefficients mid-bit. Although this may slightly increase the bit period, it enables the Tx to reach otherwise unreachable Rx.

III. Hardware Prototyping

Tags transmit by reflecting the exciter's signal and modulating data bits on it, while they receive using a passive envelope detector. For transmission, the antenna connects to m terminating impedances (Z^i) via an RF switch ($i = 1 \ldots m$), producing reflection coefficients (Γ^i) with amplitude $|\Gamma^i|$ and phase $\angle\Gamma^i$ [2]. When the switch selects Z^i, a fraction $|1-\Gamma^i|$ of the incident signal is reflected with a phase offset $\angle(1-\Gamma^i)$. For simplicity, we assume $|1-\Gamma^i|$ is constant across all i. The

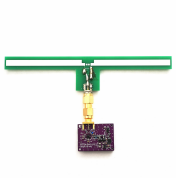

(a) With antenna attached

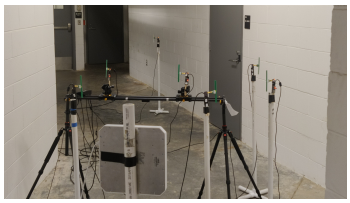

(b) Experimental Setup

Fig. 4: (a)Tag prototype built using discrete components for experimental evaluation. (b) Experimental setup used in the paper.

impedance angles ($\angle(1-\Gamma^i)$) are pre-designed to span $-\pi$ to π. The switch is managed by the tag's processing logic. For reception, the tag employs an analog envelope detector [16], similar to what is used in RFID tags, followed by an ADC for voltage measurement. The general design approach is similar to that in [6]. Figure 3 shows a block diagram of the tag.

We built a prototype circuit using commodity components on a PCB (Figure 4) to implement the backscatter transmitter and receiver. A 915MHz dipole antenna connects via an SMA connector. The RF switch uses Skyworks Sky13418, while the envelope detector is a two-stage Dickson rectifier with SMS7630 Schottky diodes. A unity-gain amplifier and an 80 kHz low-pass filter process the signal before passing it to an ADC (ADS8860) for fine-grain measurements. An ESP32 microcontroller controls the switch, samples the ADC, and transmits data to a computer via USB. Although the discrete components are not energy-efficient, limiting the prototype to external power, an ASIC implementation will reduce power consumption to the order of μW or lower [17], [6]. The exciter is a 915MHz CW signal generator emitting 12.9 dBm power, connected to a 6 dBi circularly polarized patch antenna. Both the patch antenna and tags are mounted on plastic stands (Figure 4(b)).

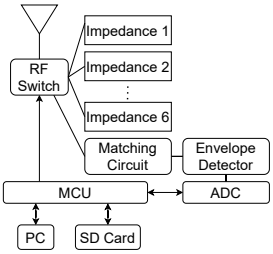

Fig. 3: Block diagram of a tag.

IV. Experimental Evaluation

We evaluated both collaborative backscatter schemes using a 7-tag network distributed over $10\,m^2$. Five topologies were tested by rearranging the tag and exciter locations (only two are shown for brevity). Although the network is small, it effectively illustrates the principles. As shown in the results, performance gains saturate after adding a few well-placed helpers, and expanding the network further provides little scientific value.

For each topology, an exhaustive measurement set was collected to evaluate the heuristic algorithms. Every combination of Tx-Rx tag pairs was tested with all possible helper subsets.

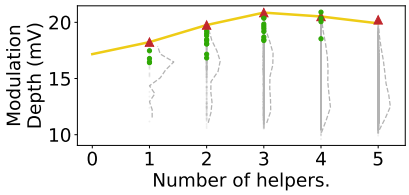

(a)

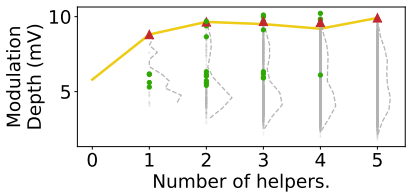

(b)

Fig. 5: Evaluation results for Scheme 1 on two different topologies (a) and (b) showing the modulation depth for different numbers of helper tags. See the text for explanation.

Each subset ran through all reflection coefficient combinations (6 coefficients per tag, with a 7th for non-reflecting). The voltage at the envelope detector output was measured at the Rx tag for every configuration.

A. Evaluation of Scheme 1

Figure 5 shows the evaluation results for Scheme 1. The horizontal axis represents the number of helpers used, with '0' as the baseline (no-helper case). The light grey dotted line displays the modulation depth distribution across all helper and reflection coefficient combinations for each helper count $(1,\ldots,5)$. The range varies by topology, as helper placement relative to Tx and Rx significantly impacts performance. Green dots indicate the optimal modulation depth for each helper configuration. The number of dots corresponds to possible helper subsets (e.g., $C_2^5 = 10$ for two helpers). Some dots overlap, but their distribution highlights the importance of helper selection in determining modulation depth.

The red triangle and yellow line represent the heuristic's performance in selecting optimal helpers and reflection coefficients. The red triangle marks the best helper set and optimal coefficients (validated via exhaustive search). Ideally, it aligns with the top green dot. The yellow line represents the modulation depth achieved by the heuristic-selected reflection coefficients for the chosen helper set. Ideally, it should pass through the red triangles, which it does consistently, with only minor deviations in a few cases.

B. Evaluation of Scheme 2

Figure 5 shows the evaluation results for Scheme 2 using the 7-tag network. The horizontal axis indicates the number of tags involved in transmission, with '0' as the baseline (no-helper case). Since helpers in Scheme 2 function like the Tx, they are counted together. For example, k tags represent one Tx and $k-1$ helper tags.

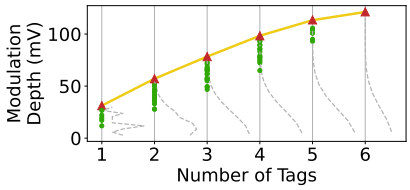

(a)

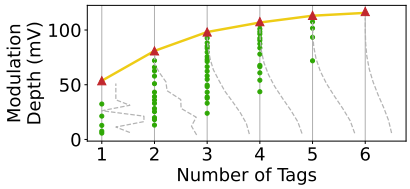

(b)

Fig. 6: Evaluation results for Scheme 2 on two different topologies (a) and (b) showing the modulation depth for different numbers of tags used in the Tx+helper tag set. See the text for explanation.

As in the previous case, the light grey dotted line in Figure 5 shows the modulation depth distribution across all possible Tx+helper sets (SH), where $|SH| = n+1$ and n range from 1 to 5. All possible reflection coefficient combinations ($\Gamma_k^i, i = 1, \ldots, m$) are considered for each tag $T_k \in SH$, with the remaining tags set to non-reflecting when $n < 5$. This again demonstrates that a range of modulation depths is possible. The green dots indicate the optimal modulation depth for each helper set configuration. The number of dots corresponds to possible helper subsets of size $|SH|$. Their distribution shows that the helper selection significantly impacts the modulation depth.

As in Scheme 1, the red triangle and yellow line in Figure 5 represent the heuristic's performance in selecting optimal helpers and reflection coefficients. The red triangle overlaps a green dot, showing that the best helper set and optimal coefficients (validated by exhaustive search) are correctly chosen. Ideally, the triangle aligns with the maximum modulation depth dot, which it consistently does. The yellow line indicates the modulation depth achieved by the heuristic-selected coefficients and helper set. It consistently follows the red triangles, demonstrating that the heuristic performs almost perfectly in Scheme 2.

The most significant takeaway in Scheme 2, however, is the tremendous gain in the modulation depth relative to Scheme 1. The gain in modulation depth is limited in Scheme 1 to 15%-70%, but in Scheme 2 it is much higher - over 100%-260%. This is expectedbecause Scheme 2 works in both directions and requires active participation from the helpers. (These numbers reflect all five topologies considered, though only two are presented here.)

V. Related Work

There is a growing literature on passive tag-to-tag communication that enables RF tags to communicate without an active receiver [4], [1], [3], [2], [7], [17]. This low-power distributed setup supports scalable deployments with dense tag networks. Unlike traditional RFID, these tags use novel backscatter modulation and passive demodulation techniques [18]. The excitation signal comes from ambient sources [1] or intentional exciters [5]. Applications include RF channel estimation [19], activity recognition [13], localization [6], and structural health monitoring [20]. See also the review in [5].

While beamforming in sensor networks is well-studied, it typically relies on active radios. RFID systems have used multiple integrated antennas on the tags for range gains [21], [22], but this approach increases tag size.

Collaborative backscatter with passive tags, as explored in [13], remains preliminary. Related studies on Reflective Intelligent Surfaces (RIS) optimize phase shifts for enhanced communication [23], [24], but RIS systems typically have localized antenna elements, unlike the distributed nature of helper tags.

VI. Conclusions

Effective communication over a network of passive tags that are able to communicate via backscattering has tremendous potential in future IoT systems. Such networks, operable using harvested power alone, can scale very well and become ubiquitous. The paper addresses the communication challenges that stem from the fact that weak modulation depths must be effectively resolved at passive receiving circuits. We have proposed mechanisms to increase the depth for easier resolution via collaborative backscattering, where a set of helper tags are recruited that alter their reflecting phases to improve the modulation depth of the link in question. We have shown via experiments and analysis that while an exhaustive search can discover the optimal parameter settings, low-cost heuristics perform almost as well.

Appendix

This appendix explains the mathematical model and the process used to select the right reflection coefficient combination for helper tags performing the CoBa scheme 1. Suppose we have $n+2$ tags. Two of them are the transmitter and receiver and n are helpers. The final equation of signal strength at the receiver can be written as

$$S_r = |S_{etr} + \sum_{i=1}^{n} S_{ehr}^i + S_{er}|, \tag{1}$$

where S_{etr} is the signal from the exciter to the transmitter to the receiver, S_{ehr}^i is the signal from the exciter to the i_{th} helper to the receiver, and S_{er} is the signal from the exciter to the receiver and which is given by

$$S_{er} = A_e A_{er} e^{j(\theta_e + \theta_{er})}. \tag{2}$$

Here, A_{er} and θ_{er} are the amplitude and phase of the exciter to receiver channel, respectively, and A_e is just a constant. The signal S_{ehr}^i can be expressed as

$$S_{ehr}^i = A_e A_{ei} |1 - \Gamma_i| A_{ir} e^{j(\theta_e + \theta_{ei} + \angle(1-\Gamma_i) + \theta_{ir})}, \tag{3}$$

where, A_{ei} and θ_{ei} are the amplitude and phase of the exciter to the i^{th} helper channel, A_{ir} and θ_{ir} are the amplitude and phase of the i^{th} helper to the receiver channel, Γ_i is the reflection coefficient of the i^{th} helper, and S_{etr} is of the form

$$S_{etr} = (S_{et} + \sum_{i=1}^{n} S^i_{eht})|1 - \Gamma_t|A_{tr}e^{j(\angle(1-\Gamma_t)+\theta_{tr})}. \quad (4)$$

The symbol Γ_t is the reflection coefficient of the transmitting tag, and A_{tr} and θ_{tr} are the amplitude and phase of the transmitter to the receiver channel, respectively. Here S_{et} can be written as:

$$S_{et} = A_e A_{et} e^{j(\theta_e+\theta_{et})}, \quad (5)$$

where A_{et} and θ_{et} are the amplitude and phase of the exciter to the transmitter channel, respectively. We express the signal S^i_{eht} by

$$S^i_{eht} = A_e A_{ei}|1 - \Gamma_i|A_{it}e^{j(\theta_e+\theta_{ei}+\angle(1-\Gamma_i)+\theta_{it})}. \quad (6)$$

The modulation depth at the receiver for a particular combination of the reflection coefficient of helper tags can be computed by plugging in all the values of the reflection coefficient of the transmitter and taking the difference between the maximum and minimum values. The modulation depth D as a function of the reflection coefficient of helper tags $(\Gamma_1, \Gamma_2, ...\Gamma_n)$ is given by

$$D(\Gamma_1, \Gamma_2, ...\Gamma_n) = \max_{<\Gamma_t>}(S_r) - \min_{<\Gamma_t>}(S_r). \quad (7)$$

Several parameters in the expression of S_r can be computed using techniques discussed in [6]. These are exciter-to-tag channel amplitude and tag-to-tag channel amplitudes and phases. However, the exciter-to-tag channel phases are unknown. Furthermore, the tag-to-tag channel phases are only known as mod pi. We experimentally collect a few values of D in order to estimate these parameters accurately. During the fitting process, three more parameters (h_1, h_2, h_3) are also calibrated to account for the noise in the readings. These parameters are used to update the values of S_r in the following way:

$$S_r = |h_1 S_{etr} + h_2 \sum_{i=1}^{n} S^i_{ehr} + h_3 S_{er}|. \quad (8)$$

After fitting, we take all the possible combinations of the reflection coefficient of helper tags $(\Gamma_1, \Gamma_2, ...\Gamma_n)$ and predict D of each of them. Subsequently, we pick three peaks of D separated by a specific number of combinations. For each of the three peaks, we choose a very small window of nearby reflection coefficient combinations. For these combinations, we collect experimental data and select the one that produces the highest modulation depth.

ACKNOWLEDGEMENT

This work was partially supported by U.S. National Science Foundation (NSF) awards 1901182 and 2038801.

REFERENCES

[1] V. Liu, A. Parks, V. Talla, S. Gollakota, D. Wetherall, and J. R. Smith, "Ambient backscatter: Wireless communication out of thin air," *ACM SIGCOMM Computer Communication Review*, 2013.

[2] J. Ryoo, J. Jian, A. Athalye, S. R. Das, and M. Stanaćević, "Design and evaluation of "BTTN": a backscattering tag-to-tag network," *IEEE Internet of Things Journal*, 2018.

[3] P. V. Nikitin, S. Ramamurthy, R. Martinez, and K. S. Rao, "Passive tag-to-tag communication," in *2012 IEEE international conference on RFID (RFID)*. IEEE, 2012, pp. 177–184.

[4] Y. Karimi, A. Athalye, S. R. Das, P. M. Djurić, and M. Stanaćević, "Design of a backscatter-based tag-to-tag system," in *2017 IEEE International Conference on RFID (RFID)*, 2017, pp. 6–12.

[5] M. Stanaćević, A. Athalye, Z. J. Haas, S. R. Das, and P. Djurić, "Backscatter communications with passive receivers: From fundamentals to applications," *ITU Journal*, vol. 1, no. 1, 2020.

[6] A. Ahmad, X. Sha, M. Stanaćević, A. Athalye, P. M. Djurić, and S. R. Das, "Enabling passive backscatter tag localization without active receivers," in *ACM SenSys*, 2021, pp. 178–191.

[7] A. Y. Majid, M. Jansen, G. O. Delgado, K. S. Yildirim, and P. Pawełłzak, "Multi-hop backscatter tag-to-tag networks," in *IEEE INFOCOM 2019-IEEE Conference on Computer Communications*. IEEE, 2019.

[8] Y. Liu, K.-W. Chin, and C. Yang, "Link scheduling for data collection in multihop backscatter IoT wireless networks," *IEEE Internet of Things Journal*, vol. 9, no. 3, pp. 2215–2226, Feb. 2022.

[9] Y.-C. Liang, Q. Zhang, J. Wang, R. Long, H. Zhou, and G. Yang, "Backscatter communication assisted by reconfigurable intelligent surfaces," *Proceedings of the IEEE*, vol. 110, no. 9, pp. 1339–1357, 2022.

[10] A. Ahmad, X. Sha, A. Athalye, S. Das, P. Djurić, and M. Stanaćević, "Collaborative backscatter based on phase channel estimation in passive RF tag networks," in *2021 IEEE International Conference on RFID Technology and Applications (RFID-TA)*, 2021, pp. 128–131.

[11] T. Lassouaoui, F. D. Hutu, Y. Duroc, and G. Villemaud, "Performance evaluation of passive tag to tag communications," *IEEE Access*, 2022.

[12] T. Lassouaoui, F. Hutu, Y. Duroc, and G. Villemaud, "Theoretical BER evaluation of passive RFID Tag-To-Tag communications," in *2020 IEEE Radio and Wireless Symposium (RWS)*. IEEE, Jan. 2020, pp. 213–216.

[13] A. Ahmad, A. Athalye, M. Stanacević, and S. R. Das, "Collaborative channel estimation in backscattering tag-to-tag networks," in *Proceedings of the 1st ACM International Workshop on Device-Free Human Sensing*, 2019, pp. 35–38.

[14] A. Ahmad, X. Sha, A. Athalye, S. R. Das, K. Caylor, B. Glisic, M. Stanacevic, and P. M. Djuric, "Dispersed passive RF-sensing for 3D structural health monitoring," *ITU Journal on Future and Evolving Technologies*, vol. 3, no. 2.

[15] "SciPy 1.11.4: Fundamental Algorithms for Scientific Computing in Python. scipy.optimize.curve — SciPy v1.11.4 manual."

[16] D. M. Dobkin, *The RF in RFID: UHF RFID in practice*. Newnes, 2012.

[17] Y. Karimi, Y. Huang, A. Athalye, S. Das, P. Djurić, and M. Stanaćević, "Passive wireless channel estimation in RF tag network," in *ISCAS*. IEEE, 2019.

[18] A. Athalye, J. Jian, Y. Karimi, S. R. Das, and P. M. Djurić, "Analog front end design for tags in backscatter-based tag-to-tag communication networks," in *IEEE ISCAS*. IEEE, 2016, pp. 2054–2057.

[19] A. Ahmad, X. Sha, A. Athalye, S. Das, P. Djurić, and M. Stanaćević, "Amplitude and phase estimation of backscatter tag-to-tag channel," in *IEEE ISCAS*. IEEE, 2022, pp. 1342–1346.

[20] M. Stanaćević, A. Ahmad, X. Sha, A. Athalye, S. Das, K. Caylor, B. Glisić, and P. M. Djurić, "RF backscatter-based sensors for structural health monitoring," in *2021 International Balkan Conference on Communications and Networking (BalkanCom)*. IEEE, 2021.

[21] J. D. Griffin and G. D. Durgin, "Gains for RF tags using multiple antennas," *IEEE Transactions on Antennas and Propagation*, 2008.

[22] Q. Wu and R. Zhang, "Intelligent reflecting surface enhanced wireless network: Joint active and passive beamforming design," in *2018 IEEE GLOBECOM*. IEEE, 2018.

[23] Y. Chen, "Performance of ambient backscatter systems using reconfigurable intelligent surface," *IEEE Communications Letters*, 2021.

[24] M. Nemati, J. Ding, and J. Choi, "Short-range ambient backscatter communication using reconfigurable intelligent surfaces," in *2020 IEEE Wireless Communications and Networking Conference (WCNC)*, 2020.